Rate constant modelling for batch flotation, as a function of gas dispersion properties

W. Kracht, G. Vallebuona *, A. Casali

Department of Mining Engineering, University of Chile, Av. Tupper 2069, Santiago, Chile

Abstract

Gas dispersion is one of the key factors in the mineral flotation process. It can be expressed by many variables such as bubble size, gas holdup, gas superficial velocity and bubble surface area flux (S_b). In particular, S_b has been found to have a strong correlation with the flotation rate constant (K). Bubble size is important because it is related with the transport capacity and with the flotation probability. It also affects the gas holdup and the bubble surface area flux. In this work bubble sizes are measured using image analysis. An empirical rate constant model is developed to relate K with S_b and other dispersion variables. This model is found to be able to predict K for two different batch flotation cells.

Keywords: Flotation rate constant; Bubble size distribution; Modelling

1. Introduction

Separation by flotation is a result of interaction of many variables, usually involving chemical, operational and machine factors. Machine factors, such as impeller speed, air flow rate and cell design do not affect the process performance in isolation, but combined they create the hydrodynamic conditions governing that performance (Finch et al., 2000). Gas dispersion is one of the key machine factors in the mineral flotation process. Usual gas dispersion properties are bubble size (d_b), gas holdup (ε_g), gas superficial velocity (J_g) and bubble surface area flux (S_b).

Gorain et al. (1995a,b, 1996) investigated the effect of gas dispersion properties on the flotation rate constant (K) in plant and pilot scale for mechanical cells over different operating conditions. These authors found (Gorain et al., 1997, 1998) that S_b was strongly related with K and that the relationship was linear, as represented by Eq. (1):

$$K = PS_b, \tag{1}$$

where P summarized the operational and chemical factors. Based on these investigations, Gorain et al. (1999) developed a model to predict S_b in mechanical cells, from operating conditions, impeller design and feed particle size. Finch et al. (2000) proposed to replace S_b by the gas holdup, ε_g. After analyzing different experimental results shown in the literature, for both mechanical and column cells, they found that S_b and ε_g were related by $S_b = 5.5\varepsilon_g$, either in laboratory, pilot or industrial scale. This relation would represent a considerable advantage, because the gas holdup is easier to measure, does not require bubble size measurements and reflects variations in both the gas flow rate and the bubble size. In other work, Hernandez et al. (2003) also found a linear K–S_b relationship, this time in the de-inking in a flotation column.

Heiskanen (2000) critically analyzed the experimental procedure and the experimental results of Gorain's

* Corresponding author.
E-mail address: gvallebu@cec.uchile.cl (G. Vallebuona).

work. He considered that these relationships must be validated with new experimental work and for different mineralogical species. Specially, the linearity of the K–S_b relationship needed to be further investigated.

Accordingly, this problem was investigated with experimental work in laboratory scale, with the objective of developing a flotation rate constant model as a function of the gas dispersion properties as well as to help in solving the controversial issues.

2. Experimental procedure

All testing was done in two batch flotation cells: Outokumpu (3.7 l) and Labtech-ESSA (4.9 l) both with an external blower. Two samples of copper sulphide ore from Codelco—Chile, Andina Division, were used. The first sample represents the rougher flotation feed, with a copper grade of 1.29%, mainly chalcopyrite (95%) and chalcocite (4%) and 80% passing size of 182 μm. The second sample represents the cleaner flotation tailing and corresponds to the scavenger–cleaner flotation feed, with grades of 2.33% Cu and 0.75% Mo and 80% passing size of 74 μm.

The flotation tests were done under conditions as used in Andina's concentrator. For the first sample, the collector used was Aero® 3894 (33 g/t), the frother was Aerofroth® 70 (38 g/t for the Outokumpu cell and 32 g/t for the Labtech-Essa cell), pH was 10.5, regulated with lime, and the concentration of solids by weight, in flotation, was 40.2% for the Outokumpu cell and 32.4% for the Labtech-Essa cell. For the second sample, the collectors used were Aero® 3894 (34 g/t) and diesel-oil (103 g/t), the frother was Aerofroth® 70 (26 g/t for the Outokumpu cell and 18 g/t for the Labtech-Essa cell), pH was 12, regulated with lime, and the concentration of solids by weight, in flotation, was 22.3% for the Outokumpu cell and 17.5% for the Labtech-Essa cell. Impeller speed and air flow rate were varied in each test.

2.1. Bubbles size measurement

To measure bubble size a bubble sampler as shown in Fig. 1 was used. This sampler was based on the Chen et al. (2001) design. The original design was improved latter on by Hernandez-Aguilar et al. (2004) to avoid bubbles overlapping. The sampler used in this work was based on the first one and consisted of a collection tube (8 mm inside diameter and 17 cm high) and a viewing chamber (3 cm wide, 5 cm high and 1.5 cm deep). The top of the viewing chamber was closed with a safety pipette filler. A black plastic piece of 1.7 cm was installed in the viewing area to provide a reference for bubble sizing.

Before sampling, the sampler was filled with water containing frother. Closing the bottom of the collecting tube, the sampler was introduced into the flotation cell and then was opened. Bubbles were collected and filmed while passing through the viewing chamber. The air accumulates at the top of the viewing chamber and the chamber becomes cloudy as the particles are released by the bubbles once they leave the liquid phase. The liquid remained clear for imaging purposes for up to 10 s. A video was obtained of which only the first 7 s, approximately, were used to assure good visibility (see Fig. 2). From this video, 38 images were captured (5 images/s) and used for measurements.

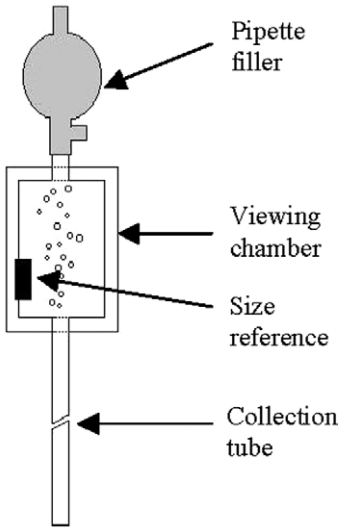

Fig. 1. Bubble sampler.

After image processing the bubble sizes were determined by image analysis, considering the mean diameter as the bubble size. These sizes had to be corrected due to the pressure difference between the sampling point into the cell and the viewing chamber. The correction was done assuming sphericity and ideal gas behaviour. The corrected sizes were grouped in size classes and the number of bubbles per class were counted. The corresponding size distribution by number (f_{i0}, number percentage in size i) was determined. Since flotation is a superficial

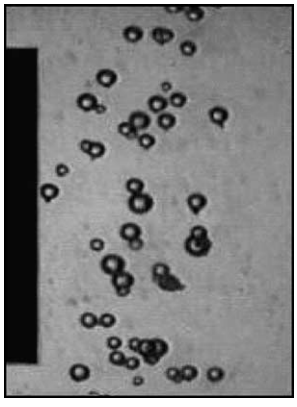

Fig. 2. Image from video.

phenomena, the size distribution by surface (f_{i2}) was calculated from the previous one according with

$$f_{i2} = \frac{x_i^2 f_{i0}}{\sum x_i^2 f_{i0}}, \quad (2)$$

where x_i corresponds to the mean bubble size in class i.

2.2. Other measurements

Besides the bubble size distributions, the gas holdup, ε_g, and the gas superficial velocity were determined for each test. The gas holdup was determined using a slurry sampler. Samples of a constant volume were weighed, with and without bubbles in it. The holdup was calculated as the weight difference divided by the weight of the sample without bubbles.

The gas superficial velocity, J_g, was determined using Eq. (3), from air flow measurements done with a flow meter and from a cell cross-sectional area, geometrically determined:

$$J_g = \frac{Q_g}{A}, \quad (3)$$

where J_g is the gas superficial velocity (cm/s), Q_g is the gas feed rate (cm^3/s) under standard conditions of pressure and temperature, and A is the useful cell cross-sectional area (cm^2).

2.3. Experimental tests

With the two flotation cells and the two samples of copper sulphide ore above mentioned, 39 experimental tests were performed. Impeller peripheral speed (Ns) and air flow rate were varied, the gas superficial velocity was calculated and the gas holdup was measured in each test. The experimental conditions for each test are presented in Table 1. The measured gas holdup, ε_g, for each test is also presented. To test reproducibility, one test was repeated three times for each cell, and the corresponding mean values of ε_g are shown in Table 1 as Or (corresponding to tests O10, O11 and O12) and Lr (corresponding to tests L08, L09 and L10), for Outokumpu and Labtech-Essa cell, respectively.

3. Experimental results

With the experimental procedure and the conditions above mentioned, the experimental tests were performed. The experimental results in terms of bubble size distributions, for some selected tests, are presented in Table 2. The bubble size distributions by surface are shown as cumulative percentage under size (F_{u2}). The size classes used in this work were more than those shown in Table 2, where only each other class is presented.

In Figs. 3–5 some of the bubble size distributions showing the effects of the experimental variables are presented. In Figs. 3 and 4, the effect of the impeller peripheral speed (Ns) on the surface bubble size distribution (F_{u2}) is shown.

As can be seen in Fig. 3, increasingly finer surface bubble size distributions were obtained at higher

Table 1
Experimental conditions

Outokumpu cell					Labtech-ESSA cell				
Test	Ns (m/s)	Q (SLPM)	J_g (cm/s)	ε_g (%)	Test	Ns (m/s)	Q (SLPM)	J_g (cm/s)	ε_g (%)
Rougher flotation feed ore									
O01	2.3	19.1	1.2	12.0	L01	2.2	9.2	0.4	9.6
O02	2.3	24.3	1.5	12.1	L02	2.2	19.8	0.8	14.7
O03	2.3	29.4	1.8	13.0	L03	2.2	30.3	1.3	18.4
O04	2.3	34.6	2.1	11.8	L04	2.4	9.2	0.4	10.9
O05	2.6	19.1	1.2	13.9	L05	2.4	19.8	0.8	14.4
O06	2.6	24.3	1.5	13.2	L06	2.4	30.3	1.3	15.0
O07	2.6	29.4	1.8	15.8	L07	2.5	9.2	0.4	11.1
O08	2.6	34.6	2.1	13.4	Lr	2.5	19.8	0.8	14.0
O09	2.9	19.1	1.2	14.9	L11	2.5	30.3	1.3	16.7
Or	2.9	24.3	1.5	14.9	L12	2.6	9.2	0.4	11.3
O13	2.9	29.4	1.8	18.3	L13	2.6	19.8	0.8	14.7
O14	2.9	34.6	2.1	17.4	L14	2.6	30.3	1.3	16.3
O15	3.2	19.1	1.2	15.3					
O16	3.2	24.3	1.5	17.0					
O17	3.2	29.4	1.8	15.6					
O18	3.2	34.6	2.1	18.8					
O19	2.8	26.9	1.7	15.2					
Scavenger–cleaner flotation feed ore									
Os1	2.6	19.1	1.2	8.0	Ls1	2.5	9.2	0.4	6.7
Os2	2.6	24.3	1.5	7.9	Ls2	2.5	19.8	0.8	9.0
Os3	2.6	29.4	1.8	7.3	Ls3	2.5	30.3	1.3	10.7

Table 2
Experimental bubble size distributions

Size (mm)	F_{u2} (%)									
	O03	O07	O09	O12	O16	Os2	L02	L06	L12	Ls2
3.1	100.0	100.0	100.0	100.0	100.0	100.0	100.0	100.0	100.0	100.0
2.9	94.6	100.0	100.0	100.0	100.0	100.0	100.0	100.0	100.0	100.0
2.7	94.6	100.0	100.0	100.0	100.0	100.0	100.0	100.0	100.0	100.0
2.5	94.6	100.0	100.0	100.0	100.0	100.0	100.0	100.0	100.0	100.0
2.3	94.6	96.3	100.0	100.0	100.0	100.0	100.0	100.0	100.0	100.0
2.1	94.6	96.3	100.0	100.0	100.0	100.0	100.0	100.0	100.0	100.0
1.9	94.6	96.3	95.4	100.0	100.0	100.0	100.0	100.0	100.0	100.0
1.7	90.9	96.3	95.4	97.6	100.0	100.0	100.0	100.0	100.0	100.0
1.5	89.3	92.6	95.4	93.6	100.0	92.8	100.0	100.0	100.0	100.0
1.3	84.6	88.7	90.7	90.5	92.8	83.7	100.0	100.0	98.5	100.0
1.1	72.3	82.1	88.9	82.4	88.5	76.7	98.0	95.7	94.0	96.2
0.9	50.9	66.4	70.1	63.9	72.4	56.9	72.0	81.3	73.1	87.1
0.7	21.1	31.7	26.4	29.5	30.6	13.3	7.1	31.6	22.4	39.0
0.5	0.8	1.8	3.5	0.4	0.2	1.7	0.1	4.7	0.8	0.4
0.3	0.0	0.1	0.6	0.0	0.0	0.2	0.0	0.8	0.0	0.0
0.1	0.0	0.0	0.1	0.0	0.0	0.0	0.0	0.1	0.0	0.0

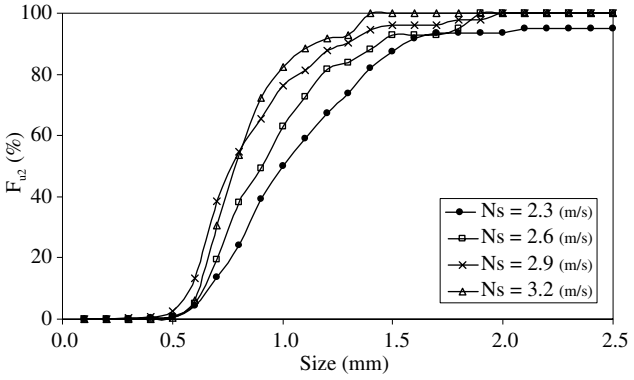

Fig. 3. Effect of impeller peripheral speed on surface bubble size distribution. Outokumpu cell, J_g = 1.5 cm/s.

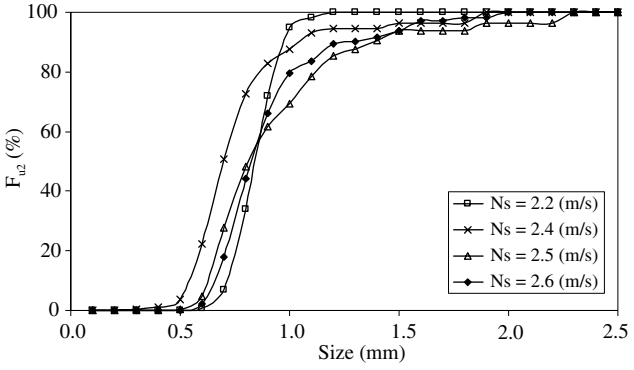

Fig. 4. Effect of impeller peripheral speed on surface bubble size distribution. Labtech-Essa cell, J_g = 0.8 cm/s.

impeller peripheral speeds. The shape of all distributions are similar, except for the highest speed, which produces a more concentrated distribution around its mean size.

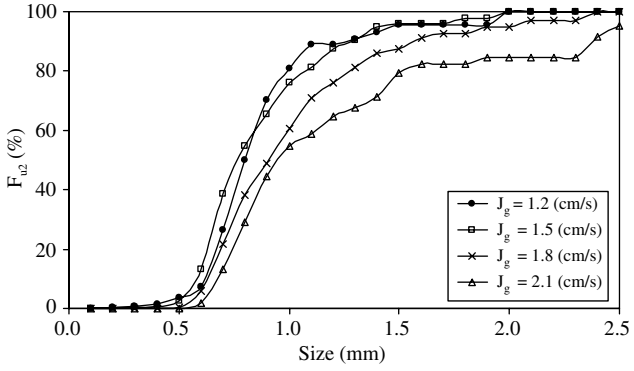

Fig. 5. Effect of gas superficial velocity on surface bubble size distribution. Outokumpu cell, Ns = 2.9 m/s.

Specially, notable is the effect of the speed on the maximum bubble size, which goes from 1.4 mm for the highest speed to almost 2.8 mm for the lowest speed.

With respect to the Labtech-Essa cell, as can be seen in Fig. 4, the results were surprisingly different. In this case the effect of the impeller peripheral speed was not clear in its trend. The speed changes the bubble size distributions but not in the expected way. Seems like the dynamic of this cell produces size distributions more concentrated around the mean size of each one, for all the tested conditions. In the OK cell instead, it is only for the highest speed where a similar size distribution was found.

In Fig. 5, the effect of the gas superficial velocity (J_g) on the surface bubble size distribution (F_{u2}) is shown.

As can be seen in Fig. 5, as the superficial velocity increases the bubble size distribution gets coarser. The shape of all distributions are similar, except for the lowest speed, which produces a more concentrated distribution around its mean size.

Table 3
Experimental kinetic parameters

Outokumpu cell				Labtech-ESSA cell			
Test	K (min^{-1})	R_∞ (%)	R^2	Test	K (min^{-1})	R_∞ (%)	R^2
Rougher flotation feed ore							
O01	0.60	89.5	0.995	L01	1.07	85.8	0.978
O02	0.58	87.7	0.991	L02	1.21	83.8	0.952
O03	0.70	88.8	0.987	L03	1.33	83.6	0.947
O04	0.83	88.6	0.983	L04	1.03	84.7	0.986
O05	0.72	90.3	0.986	L05	1.24	86.2	0.950
O06	0.86	90.9	0.982	L06	1.44	85.7	0.924
O07	0.88	90.9	0.987	L07	1.17	86.9	0.964
O08	0.86	89.3	0.983	L08	1.32	88.5	0.945
O09	0.90	90.2	0.963	L09	1.40	87.2	0.934
O10	0.84	89.3	0.984	L10	1.33	88.4	0.937
O11	0.89	91.2	0.977	L11	1.44	88.0	0.901
O12	0.94	91.2	0.988	L12	1.19	87.8	0.963
O13	0.90	91.3	0.989	L13	1.46	89.0	0.931
O14	0.96	92.1	0.970	L14	1.52	88.8	0.907
O15	0.95	91.3	0.982				
O16	0.99	91.6	0.988				
O17	1.04	91.1	0.981				
O18	1.13	91.6	0.975				
O19	0.85	90.2	0.989				
Scavenger–cleaner flotation feed ore							
Os1	0.29	80.2	0.991	Ls1	0.29	84.5	0.985
Os2	0.30	81.3	0.984	Ls2	0.35	86.1	0.980
Os3	0.33	83.4	0.981	Ls3	0.47	87.1	0.976

3.1. Kinetic results

The flotation kinetic results of the 39 experimental tests were fitted to the first-order rate equation (Wills, 1997) and all the tests were found with a reasonably good fit. The results in terms of the kinetic parameters K (first-order rate constant, time^{-1}) and R_∞ (maximum theoretical flotation recovery), together with the correlation coefficient (R^2) for each fitting, are shown in Table 3.

As was previously mentioned, one test was repeated three times for each cell, and these are O10, O11 and O12 for the Outokumpu cell and L8, L9 and L10 for the Labtech-Essa cell. The errors were 6% and 3% in K values for Outokumpu and Labtech-Essa cell, respectively, and 1% in R_∞ for both cells.

4. Modelling

As was mentioned, the objective of this work was to develop a flotation rate constant model as a function of the gas dispersion properties. In the case of the bubble size distribution it is necessary to represent it with a model, so that its parameters could be included as possible variables in the flotation rate model.

4.1. Bubble size distribution model

As was mentioned before, since flotation is a superficial phenomena, the size distribution by surface was modelled. To determine the best structure of the model, 24 known equations were tested for goodness-of-fit. These equations have been already used either to represent particle size distributions or classification efficiencies or heavy media partition curves.

All models were fitted to the experimental results. The procedure was to minimize the sum of squares of the residuals between modelled and experimental values, for the bubble size distribution by surface expressed as percentage in size i (f_{i2}) as well as cumulative percentage under size (F_{u2}). Both correlation coefficients ($R^2_{f_i}$ and $R^2_{F_u}$) were determined, using them as indicators of the goodness-of-fit for each model.

The best model found was an empirical equation (King, 2001) also used to represent partition curves in heavy media separation, adapted and expressed as cumulative percentage under size. This model is presented in Eq. (4):

$$Fu_2(x) = 100 \exp\left(-0.693\left(\frac{x}{x_{50}}\right)^{-\lambda}\right), \tag{4}$$

where x_{50} corresponds to the size under which is the 50% of the surface of bubbles and λ is a parameter to be adjusted. In this case λ is a parameter that represents the bubble size distribution shape. Higher the λ value more narrow the distribution, i.e., more concentrated around the mean size x_{50}.

Model parameters and correlation coefficients for all tests are shown in Table 4. In Figs. 6 and 7 modelled and

experimental bubble size distributions are presented, for tests showing average goodness-of-fit, for Outokumpu and Labtech-Essa cell, respectively. In Fig. 6 the bubble size distribution corresponding to the test O06 is presented. Fig. 7 shows the corresponding distribution for the L07 test.

4.2. Rate constant model

Correlation between the flotation rate constant and the gas dispersion variables was studied, searching for a model linear in the parameters. The model structure was developed with a stepwise regression method (Casali et al., 1998). This method determines the set of components, from a list of candidate components, in order to give the best model for the desired variable. The procedure starts with the selection of the candidate component that is most closely correlated to the output, thus establishing a first partial model. The residue from this partial model is correlated to the remaining candidate variables. In each subsequent step, the variable selected is the one giving the largest partial correlation to the residue from the previous step, and this is calculated from performing a multiple-linear regression with the variables previously included. Before including each new term, all the selected terms are tested for their statistical significance. Since a prediction-error estimator is used to estimate the coefficients, the estimates have an estimated prediction-error deviation. The ratio between this deviation and the coefficient, for each included component, is used to decide the inclusion of the new term. If for any component the ratio exceeds a given value (0.5 in this

Table 4
Bubble size distribution model parameters

Outokumpu cell					Labtech-ESSA cell				
Test	x_{50} (mm)	λ	$R^2_{F_u}$	$R^2_{f_i}$	Test	x_{50} (mm)	λ	$R^2_{F_u}$	$R^2_{f_i}$
Rougher flotation feed ore									
O01	0.83	3.7	0.998	0.998	L01	1.00	2.9	0.989	0.783
O02	0.99	3.3	0.998	0.998	L02	0.85	9.6	0.997	0.974
O03	0.89	3.5	0.998	0.998	L03	0.82	6.3	1.000	0.996
O04	1.04	2.2	0.992	0.992	L04	0.74	9.0	0.998	0.986
O05	0.81	3.3	0.996	0.996	L05	0.70	5.2	0.999	0.980
O06	0.88	3.7	0.999	0.999	L06	0.77	6.9	0.998	0.972
O07	0.80	4.0	0.999	0.999	L07	0.80	6.1	0.997	0.937
O08	1.16	2.5	0.990	0.990	Lr	0.91	3.5	0.993	0.866
O09	0.81	5.0	0.998	0.998	L11	1.08	3.6	0.997	0.896
Or	0.77	4.4	0.998	0.998	L12	0.79	6.4	0.999	0.989
O13	0.89	3.3	0.999	0.999	L13	0.83	5.6	0.999	0.975
O14	0.99	2.8	0.990	0.990	L14	0.79	4.1	0.994	0.862
O15	0.80	3.9	0.998	0.998					
O16	0.78	5.1	0.999	0.999					
O17	0.87	3.6	0.998	0.998					
O18	0.86	3.0	0.996	0.996					
O19	0.83	5.7	0.998	0.998					
Scavenger–cleaner flotation feed ore									
Os1	0.86	4.1	0.996	0.891	Ls1	0.91	4.9	0.997	0.936
Os2	0.88	4.9	0.997	0.902	Ls2	0.74	7.1	0.999	0.986
Os3	0.98	3.9	0.997	0.924	Ls3	0.90	3.7	0.999	0.979

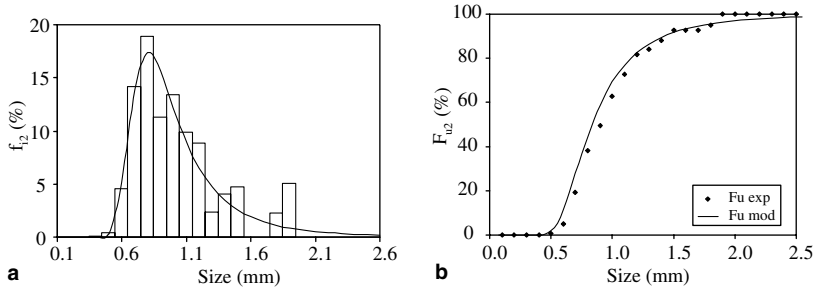

Fig. 6. Bubble size distribution by surface. Outokumpu cell, Ns = 2.6 m/s, J_g = 1.8 cm/s. (a) Experimental histogram and model line, f_{i2}. (b) Cumulative distribution, F_{u2}.

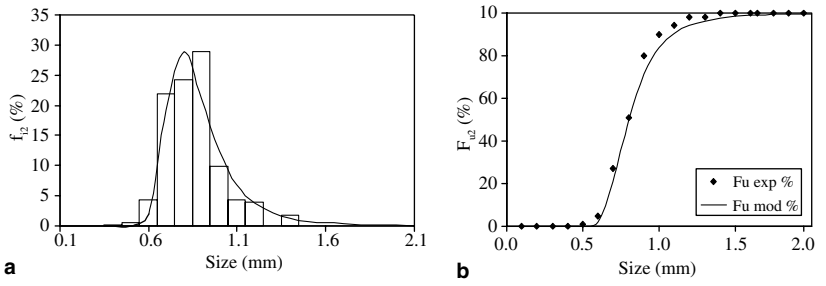

Fig. 7. Bubble size distribution by surface. Labtech-ESSA cell, Ns = 2.5 m/s, J_g = 0.4 cm/s. (a) Experimental histogram and model line, f_{i2}. (b) Cumulative distribution, F_{u2}.

work) then it is not included. When there is no remaining term to be selected, the model structure is complete.

The candidate components were all the dispersion properties (d_b, ε_g, J_g and S_b), the impeller peripheral speed (Ns), the parameters of the bubble size distribution model (λ and x_{50}) and many characteristic sizes of the bubble size distribution such as x_{80}, x_{50}, x_{75}, etc. Combinations of these components, with some phenomenological meaning were also proposed. In total more than 100 candidate components were considered.

As bubble size d_b, the d_{32} diameter was used, which corresponds to the Sauter mean diameter (Gorain et al., 1997), determined from the experimental bubble size distribution. The bubble surface area flux (S_b) was determined from Eq. (5). The calculated d_{32} and S_b values for all the tests, are shown in Table 5.

$$S_b = \frac{6J_g}{d_{32}}. \tag{5}$$

With this procedure two alternative model structures were found. The first one was determined using the experimental data obtained with the Outokumpu cell for the rougher flotation feed ore, leaving out test O19 for validation purposes. This model is presented as Eq. (6):

$$K = C_0 + C_1 \mathrm{Ns} S_b + C_2 Ns + C_3 x_{80}^3. \tag{6}$$

The second one was determined using the experimental data obtained with the Labtech-ESSA cell for the rougher flotation feed ore, leaving out test L05 for validation purposes. This model is presented as Eq. (7):

$$K = C_0 + C_1 \mathrm{Ns}\, \varepsilon_g + C_2 \lambda + C_3 d_{10}, \tag{7}$$

where d_{10} corresponds to the number mean diameter and C_k ($k = 0, 1, \ldots, 3$) are the model coefficients.

Ideally, a good model should be able to represent any cell, with different ores, just changing the parameters. To find out if this is true and to select the best model, each model structure was tested for goodness-of-fit considering four data sets. The data set where the model structure was generated (a particular cell using the rougher flotation feed ore), the data set with the same ore but the other cell (cross-validation), and two additional, but limited, data sets using the scavenger–cleaner flotation feed ore. To evaluate the statistical significance of each model in each case, the ratio between the estimated prediction-error deviation ($se(C_k)$) and the coefficient value (C_k) was calculated.

To compare the quality of both models their fitting results are presented in Table 6. For each model and each data set, the values of the model coefficients are shown. Also two statistical indicators are shown: the correlation coefficient (R^2) and the maximum value of the prediction-error deviation ratio (ϕ), as presented in Eq. (8). This ratio allows to determine if a variable makes a significant contribution to the full model. The decision is based on the F-test and considers that for a 97.5% of confidence, a variable contributes to the model if $\phi < 0.5$ (Himmelblau, 1970).

Table 5
Bubble surface area flux (S_b)

Outokumpu cell			Labtech-ESSA cell		
Test	d_{32} (mm)	S_b (s^{-1})	Test	d_{32} (mm)	S_b (s^{-1})
Rougher flotation feed ore					
O01	0.97	73.6	L01	1.24	18.9
O02	1.12	80.4	L02	0.84	59.3
O03	1.04	105.0	L03	0.85	89.6
O04	1.24	103.5	L04	0.73	32.1
O05	0.95	75.2	L05	0.76	65.5
O06	0.97	92.8	L06	0.77	99.0
O07	0.90	121.3	L07	0.81	28.9
O08	1.34	95.8	L08	0.93	53.5
O09	0.87	82.1	L09	1.13	44.1
O10	0.86	104.7	L10	1.37	36.4
O11	0.87	103.5	L11	1.30	58.6
O12	0.88	102.3	L12	0.81	28.9
O13	1.01	108.1	L13	0.90	55.3
O14	1.21	106.1	L14	0.96	79.4
O15	0.89	80.2			
O16	0.83	108.4			
O17	0.95	114.9			
O18	1.02	125.9			
O19	0.89	111.9			
Scavenger–cleaner flotation feed ore					
Os1	1.00	71.4	Ls1	0.97	24.1
Os2	0.94	95.7	Ls2	0.75	66.4
Os3	1.09	100.2	Ls3	1.01	75.4

Table 6
Rate constant model coefficients and goodness-of-fit statistical indicators

Data set		Model coefficients				Statistical indicators	
Cell	Ore	C_0	C_1	C_2	C_3	R^2 (%)	ϕ
Model equation (6)							
Outokumpu	Rougher feed	−0.218	0.0010	0.270	0.018	91.6	0.4
Labtech-ESSA	Rougher feed	−0.696	0.0020	0.667	0.032	92.6	0.3
Outokumpu	Scav–cl. feed	0.128	0.0002	0.030	0.021	–	–
Labtech-ESSA	Scav–cl. feed	0.014	0.0010	0.045	0.071	–	–
Model equation (7)							
Outokumpu	Rougher feed	0.616	0.013	−0.027	−0.275	81.7	0.9
Labtech-ESSA	Rougher feed	0.996	0.021	−0.023	−0.373	90.5	0.5
Outokumpu	Scav–cl. feed	−0.970	0.045	0.047	0.155	–	–
Labtech-ESSA	Scav–cl. feed	0.261	0.015	−0.021	−0.125	–	–

$$\Phi = \max\left\{\left|\frac{se(C_k)}{C_k}\right|\right\}. \quad (8)$$

As can be seen in Table 6, both models show a good fitting ($R^2 > 90\%$ and $\phi \leqslant 0.5$) for the data where their structures were determined. However, when they are tested in a cross-validation with the other data set corresponding to the same ore, the quality of the first model (Eq. (6)) is even better ($R^2 > 92\%$ and $\phi < 0.4$), but the second model (Eq. (7)) shows a performance not good enough ($R^2 < 82\%$ and $\phi = 0.9$). Additionally, when both models are tested with data sets corresponding to other ore (scavenger–cleaner flotation feed), even if the statistical indicators cannot be determined due to the limited amount of data, it can be observed that in the case of the first model all the coefficients keep the sign for both data sets (model toughness), but for the second model the sign of most of the coefficients changes (model instability).

Considering all the results above mentioned, the first model (Eq. (6)) was selected as the more appropriate flotation rate constant model. This four parameters model is able to predict the rate constant for both cells and for both ores tested.

The model quality can be observed in Fig. 8, for the data sets corresponding to the rougher flotation feed ore, for both cells. The correlation coefficients are those presented in Table 6. In both cases a test was not considered in the model structure determination, so can be used for validation purposes. The prediction of both validation tests are shown as filled circles in the corresponding part of Fig. 8.

As can be seen in Fig. 8 the fit and the prediction quality (validation tests) of the model, for both data sets is good enough, with correlation coefficients of 91.6% and 92.6% for the Outokumpu cell data set and the Labtech-Essa cell data set, respectively.

Fig. 9 shows how the model predicts the rate constant. In this figure the K versus S_b relationship is presented, with the coefficients corresponding to the Outokumpu cell and rougher flotation feed data set. Since this is a 3-variable problem, results are presented separated by the value of the impeller peripheral speed (Ns). Two groups of results are presented: (a) Ns = 2.3 (m/s) and (b) Ns = 3.2 (m/s); which are the extreme values considered in this work. In each one of them, four pairs of points are shown. Each pair corresponds to a given combination of S_b and x_{80}. In each pair one point corresponds to the experimental value (filled symbol) and the other to the modelled value.

As can be seen in Fig. 9, a K–S_b relationship was found. If linearity is assumed, the slope changes with Ns and the constant changes strongly with Ns. Linearity is more evident for higher impeller speeds than for lower

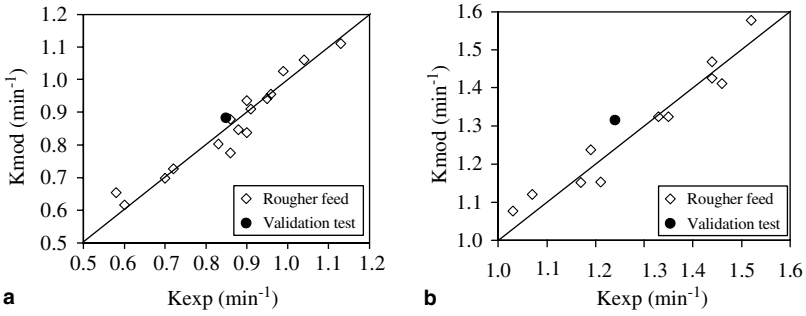

Fig. 8. Correlation between estimated (Eq. (6)) and experimental rate constants for all rougher flotation tests, including a validation test, obtained from (a) Outokumpu cell and (b) Labtech-Essa cell.

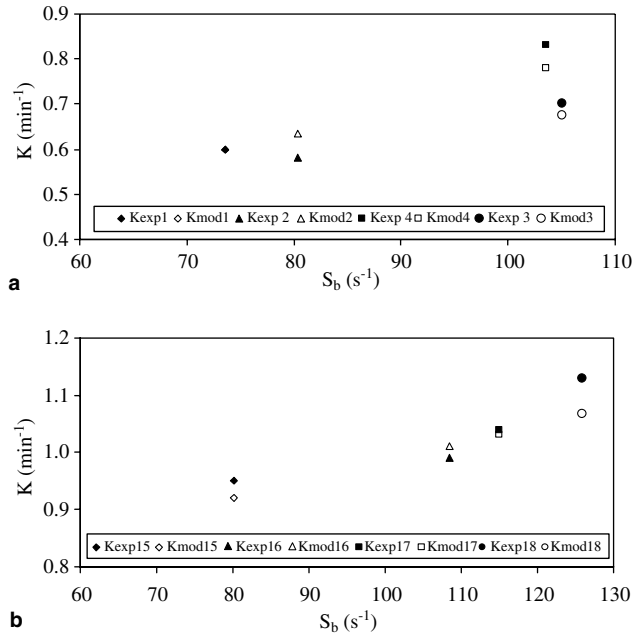

Fig. 9. K experimental and model as a function of S_b. Model prediction for two impeller speed fixed conditions: (a) Ns = 2.3 m/s and (b) Ns = 3.2 m/s with x_{80} from own test.

ones, where at higher S_b values the linearity is not longer true. The differences between experimental and modelled K values are lower than 10% of the mean value and represent an average error of 4%, lower than the experimental error for the K values (6%).

5. Conclusions

It was possible to measure bubble sizes using a bubble sampler based on the Chen et al. (2001) design. The sizes were grouped in size classes and the number of bubbles per class were counted. The corresponding size distribution by number (f_{i0}) was determined and since flotation is a superficial phenomena, the size distribution by surface (f_{i2}) was calculated.

For the Outokumpu cell, increasingly finer surface bubble size distributions were obtained at higher impeller peripheral speed (Ns). The shape of all distributions were similar, except for the highest speed, which produces a more concentrated distribution around its mean size. Specially, notorious was the effect of the speed on the maximum bubble size, which goes from 1.4 mm for the highest speed to almost 2.8 mm for the lowest speed. For the Labtech-Essa cell, the results were surprisingly different. The effect of Ns was not clear in its trend. The dynamic of this cell produced size distributions more concentrated around the mean size, for all the tested conditions. In the OK cell instead, it is only for the highest speed where a similar size distribution was found.

The bubble size distribution by surface was modelled. The best model found ($R^2 > 99\%$ for the cumulative distribution) was an empirical equation (King, 2001), adapted and expressed as cumulative percentage under size. One of its two parameters corresponds to x_{50}, the size under which is the 50% of the surface of bubbles. The other parameter, λ, represents the bubble size distribution shape. Higher the λ value more narrow the distribution, i.e., more concentrated around the mean size x_{50}.

A flotation rate constant model as a function of the gas dispersion properties was developed, based on experimental work at laboratory scale with samples from a copper sulphide ore. The model structure was developed with a stepwise regression method. With this procedure, the best structure found (Eq. (6)) was a function of the bubble surface area flux (S_b), the impeller peripheral speed (Ns) and the size under which is the 80% of the surface of bubbles (x_{80}). The model correlation coefficient, R^2, was 0.916 for the data where its structure was determined and was 0.926 when tested in a cross-validation with the other data set. The statistical significance of the model coefficients, in terms of the maximum value of the prediction-error deviation ratio, was lesser than 0.4 in both cases.

The modelled K–S_b relationship was analyzed. As it is shown in Fig. 9, a linear K–S_b relationship was found, where the slope changes with Ns and the constant changes strongly with Ns. Linearity is more evident for higher impeller speeds than for lower ones, where at higher S_b values the linearity is not longer true. The differences between experimental and modelled K values are lower than the experimental error for the K values.

Finally, it can be concluded that an empirical model of the flotation rate constant was developed, able to predict K with a lower than 10% error, for two different batch flotation cells, as a function of S_b and other variables. This model agrees, but not absolutely, with the linearity of the K–S_b relationship, at least between the range of the experimental variables.

Acknowledgement

The research and development leading to this paper has been financed by Chilean National Science and Technology Council (CONICYT), Project FONDECYT 1030807.

References

Casali, A., González, G., Torres, F., Vallebuona, G., Castelli, L., Gimenez, P., 1998. Particle size distribution soft-sensor for a grinding circuit. Powder Technology 99, 15–21.

Chen, F., Gomez, C.O., Finch, J.A., 2001. Technical note: Bubble size measurement in flotation machines. Minerals Engineering 14 (4), 427–432.

Finch, J., Xiao, J., Hardie, C., Gomez, C., 2000. Gas dispersion properties: bubble surface area flux and gas holdup. Minerals Engineering 13 (4), 365–372.

Gorain, B., Franzidis, J., Manlapig, E., 1995a. Studies on impeller type, impeller speed and air flow rate in an industrial scale flotation cell, Part 1: effect on bubble size distribution. Minerals Engineering 8 (6), 615–635.

Gorain, B., Franzidis, J., Manlapig, E., 1995b. Studies on impeller type, impeller speed and air flow rate in an industrial scale flotation cell, Part 2: effect on gas holdup. Minerals Engineering 8 (12), 1557–1570.

Gorain, B., Franzidis, J., Manlapig, E., 1996. Studies on impeller type, impeller speed and air flow rate in an industrial scale flotation cell, Part 3: effect on superficial gas velocity. Minerals Engineering 9 (6), 639–654.

Gorain, B., Franzidis, J., Manlapig, E., 1997. Studies on impeller type, impeller speed and air flow rate in an industrial scale flotation cell, Part 4: effect of bubble surface area flux on flotation performance. Minerals Engineering 10 (4), 367–379.

Gorain, B., Napier-Munn, T., Franzidis, J., Manlapig, E., 1998. Studies on impeller type, impeller speed and air flow rate in an industrial scale flotation cell, Part 5: validation of K–S_b relationship and effect of froth depth. Minerals Engineering 11 (7), 615–626.

Gorain, B., Franzidis, J., Manlapig, E., 1999. The empirical prediction of bubble surface area flux in mechanical flotation cells from cell design and operating data. Minerals Engineering 12 (3), 309–322.

Heiskanen, K., 2000. On the relationships between flotation rate and bubble surface area flux. Minerals Engineering 13 (2), 141–149.

Hernandez, H., Gómez, C., Finch, J., 2003. Gas dispersion and de-inking in a flotation column. Minerals Engineering 16 (8), 739–744.

Hernandez-Aguilar, J., Coleman, R., Gomez, C., Finch, J., 2004. A comparison between capillary and imaging techniques for sizing bubbles in flotation systems. Minerals Engineering 17 (1), 53–61.

Himmelblau, D., 1970. Process Analysis by Statistical Methods, first ed. Sterling Swift.

King, R.P., 2001. Modeling & Simulation of Mineral Processing System, first ed. Butterworth-Heinemann, Oxford.

Wills, B.A., 1997. Mineral Processing Technology, sixth ed. Pergamon Press, Oxford.